Turkish Journal of Physics

http://journals.tubitak.gov.tr/physics/

Research Article

Turk J Phys
(2019) 43: 531 – 539

doi:10.3906/fiz-1907-1

Two-dimensional Ti_2C monolayer (MXene): surface functionalization, induced metal, semiconductor transition

Berna AKGENÇ*
Department of Physics, Faculty of Science, Kırklareli University, Kırklareli, Turkey

Received: 01.07.2019 • **Accepted/Published Online:** 23.08.2019 • **Final Version:** 21.10.2019

Abstract: Recently, two-dimensional (2D) transition metal carbides and nitrides known as MXenes, have gained a lot of attention because of their tunable electronic and magnetic properties depending on surface functionalization. In the present work, the structural, electronic, and magnetic properties of both T and H phases of bare Ti_2C and fully surface terminated Ti_2CT_2 (T = -F, = O, -OH) are calculated using a set of first principles calculations. The ground state structures of Ti_2CT_2 are computed in two and four different configurations for both H and T phases, respectively. We demonstrate that while H phase of Ti_2C exhibits half-metallic behavior with magnetic moments of 2 μ_B per formula unit, it displays metallic behavior with magnetic moments of 1.27 μ_B, 0.25 μ_B per formula unit, and semiconductor behavior with 0.35 eV band gap in -F, -OH, and =O surface functionalization, respectively. We also show that while T phase of Ti_2C exhibits metallic behavior with magnetic moment of 1.89 μ_B per formula unit, it stays in metallic nonmagnetic behavior in both -F and -OH. Meanwhile, it displays semiconductor behavior with 0.25 eV band gap in -O surface functionalization. We expect that our results can advance the future applications of MXenes from energy storage to spintronic.

Key words: 2D materials, density functional theory, MXenes, Ti_2C, electronic and magnetic properties, surface functionalization

1. Introduction

Two-dimensional (2D) freestanding materials show unique properties that differ from those of their conventional bulk (3D) precursors because they lack a degree of freedom. The first 2D material, graphene, was discovered in 2004 by mechanical exfoliation method [1, 2]. This method is the most economical way to achieve single layer material. The alternative of 2D materials [3–6], such as hexagonal BN [7], transition metal oxides [8] and transition metal dichalcogenides (TMDs) [9, 10] have also been synthesized by the same method. Naguib et al. reported that they obtained a compose of a few Ti_3C_2 layers and canonical scrolls produced by exfoliation of Ti_3AlC_2 in hydrofluoric acid [11] at room temperature. These new 2D materials occur when Al atoms are extracted from Ti_3AlC_2, which was proposed to be called "MXene" to emphasize its graphene-like morphology. MXenes has just recently entered the research area as a new member of 2D materials family. Their general formula consist of $M_{n+1}AX_n$ (n=1,2,3), M, A, and X represent early transition metal, A-group elements, and C and/or N, respectively. They were produced by selectively etching "A" layers out of the MAX bulk. After their exfoliation from the MAX phase, MXenes are fully surface-terminated by functionalized groups.

*Correspondence: berna.akgenc@klu.edu.tr

After the synthesis of Ti_3C_2, almost 30 MXenes have been also experimentally discovered, and dozens have been theoretically predicted [12–15] The exfoliation process of MAX phases is still the main challenge of getting 2D monolayer MXenes. Lei et al. considered three different structures which are monolayer alpha -Mo_2C, 1T-Mo_2C, and 2H-Mo_2C [16]. Their calculations indicate that 2H-Mo_2C is determined to be energetically most favorable among these three. To our knowledge, they put forward the physical and thermal properties of 2H -Mo_2C in the literature for the first time. Motivated by the study, we investigated the electronic and magnetic properties of bare Ti_2C and fully surface terminated Ti_2CT_2 for both H and T phases.

Surface functionalization is a critical issue on electronic, magnetic, and their tunable properties of MXenes. There are several studies that can be cited as examples: Champagne et al. [17] investigated electronic properties and dynamical stabilities, both bare V_2C and fully surface terminated V_2CT_2 from first-principles calculations. They showed that pristine V_2C shows metallic behavior and keeps its metallic behavior in all surface groups. Si et al. [18] showed intrinsic half-metallicity in bare Cr_2C due to mobility of d electrons of Cr atoms. They also showed a ferromagnetic-antiferromagnetic transition which stems from surface functionalization groups (F, OH, H, or Cl), band gap of the semiconductor can be controlled by changing the type of functional groups. The effect of surface functionalization groups was also investigated by Zhang et al. [19]. They reported that surface functionalization groups are crucially important considering their unsaturated surface which allows electron-phonon interaction.

2. Computational methodology

The structural, electronic, and magnetic properties of all the considered systems were performed by first-principles calculations using density functional theory (DFT), as implemented in the Vienna ab initio simulation package (VASP) code [20, 21]. The exchange-correlation potential energies were described by the generalized gradient approximation (GGA) [22] of Perdew-Burke-Ernzerhof (PBE) [23] functional. The density functional theory (DFT), D2 method for Grimme, was used for the GGA function with van der Waals (vdW) correction [24].

After testing of significant input parameters, structural calculations were performed by using the following parameters: The energy cutoff value for plane-wave basis set was taken to be 600 eV. The total energy was minimized until the energy between consecutive steps in the iterations variation was less than 10^{-5} eV. Hellmann–Feynman force convergence criterion was taken to be 10^{-5} eV. Fermi level Gaussian smearing factor was taken as 0.05 eV. $16\times16\times1$ k-point grid in Γ-centered mesh for the primitive unit cell was selected for the Brillouin zone (BZ) integration. The vacuum spacing was selected 20 Å between two adjacent layers to avoid interactions between the periodic images of slabs in the the z-direction. Ti, C, F, O, and H atoms were treated as $3s^2 3p^6 3d^3 4s^1$, $2s^2 2p^2$, $2s^2 2p^5$, $2s^2 2p^4$, and $1s^1$ as valence electrons, respectively.

3. Results

3.1. Structural properties

We started with fully relaxed geometry optimization of pristine H phase Ti_2C. The ground state structure of pristine H phase Ti_2C is found to be hexagonal crystal structure as shown in Figure 1a. a = b = 3.05 Å are found as equilibrium lattice parameters. To our knowledge, there is no report of performing the structural properties of H phase Ti_2C. After we got ground-state crystal structure of pristine Ti_2C, we continued functionalization

of Ti_2C MXene structure with T = F,O,OH. We considered two different configurations of functional groups for *H* phases: functionalized groups stay at the top site of Ti and C atoms shown respectively in Figures 1b and 1c. Structural parameters and formation energies of these structures are given in Table 1.

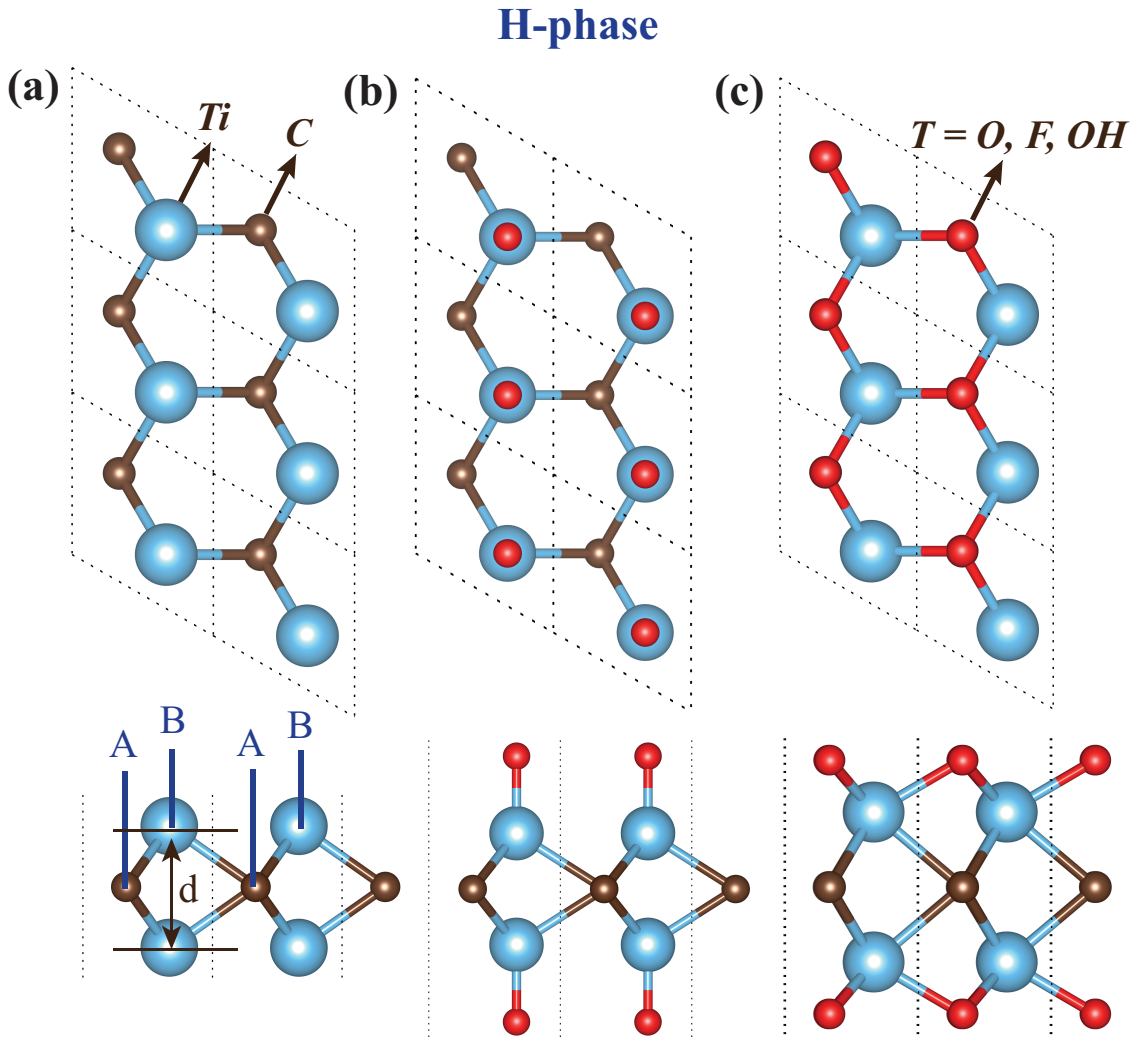

Figure 1. Systematic illustration of *H* phases of (a) pristine Ti_2C and surface terminated functionalization Ti_2CT_2 MXene systems: top and side views of (b) MD - I and (c) MD - II, respectively. Titanium, carbon, and functional groups represented in blue, brown, and red, respectively.

Formation energies are calculated to get the most stable configuration using the following formula:

$$\Delta H_f = E_{tot}(Ti_2CT_2) - E_{tot}(Ti_2C) - E_{tot}(T_2), \tag{1}$$

where $E_{tot}(Ti_2CT_2), E_{tot}(Ti_2C)$, $E_{tot}(T_2)$ total energy of fully surface terminated Ti_2CT_2, total energy of pristine Ti_2C and total energy of F_2, O_2 or $(OH)_2$, respectively. MXenes surfaces are assumed that there were no remaining bond as pending [25]. The structural parameters and calculated formation energy are reported in Tables 1 and 2.

Table 1. Structural parameters and formation energies for unterminated H-Ti_2C and surface chemically functionalized systems called MD-I and MD-II.

	Model	Lattice Parameter a (Å)	Thickness d (Å)	Magnetic moment (μ_B)	Formation Energy (eV)
H-Ti_2C		3.05	2.47	2.00	0
H-Ti_2CF_2	MD-I	3.10	2.59	1.73	–11.21
	MD-II	2.95	2.65	1.27	–13.40
H-Ti_2CO_2	MD-I	3.28	2.41	0.00	–11.22
	MD-II	2.96	2.89	0.00	–15.23
H-$Ti_2C(OH)_2$	MD-I	3.12	2.585	1.33	–8.31
	MD-II	3.00	2.58	0.25	–11.00

We used the same method in the computation of T phase Ti_2C for calculating fully relaxed geometry optimization as in the computation of H phase Ti_2C. The ground-state structure of pristine T phase Ti_2C is also found to be hexagonal as shown in Figure 2a. The unit cell includes three atoms; two titanium and one carbon are located at *(1/3, 2/3, z)*, *(2/3, 1/3, -z)*, and *(0, 0, 0)* on the Wyckoff sites. A, A‘, and B sites was selected fcc and hcp sites located on the top of Ti atom and fcc site located on the top of C atom, respectively. The equilibrium lattice parameters for T phase Ti_2C is found a = b = 3.08 Å. The lattice parameter of T phase Ti_2C is also verified by the previous studies; a = 3.083 Å [26] and a = 3.078 Å [27]. Our results show that while lattice parameters decreases, Ti–Ti atomic distance (thickness) increases. After we got ground-state crystal structure of pristine T phase Ti_2C, we continued functionalizing Ti_2C MXene structure with T = F, O, OH. To determine the ground state for T phase Ti_2CT_2, we calculated formation energies with Equation 1 in all functional groups which are listed in Table 2. Functionalization configurations are created according to the position of surface groups. We introduced four configuration models. In model MD-I, two functionalized groups are located on the top of the Ti atoms as shown in Figure 2b. In model MD-II, two functionalized groups are positioned on the top of A hollow site as shown in Figure 2c while one functionalized group is positioned on the top of A hollow site and second functionalized same type on the top of B hollow site in model MD-III as shown in Figure 2d. Finally, in model MD-IV, two functionalized groups are positioned on the top of hollow site B as shown in Figure 2e.

As seen in Tables 1 and 2, MD-II and MD-III configurations have the lowest formation energy for H and T phases, respectively. Total energies of H and T phases are found as –24.20 eV and –25.39 eV per unit cell. Clearly, T phase of Ti_2C is the most stable. The structural stability of the H and T phases was estimated by comparing their relative total energies. Clearly, relative total energy is 1.19 eV per unit cell and H-T phase transition may possible. Further studies are needed to confirm this and it should be investigated deeply.

3.2. Electronic and magnetic properties

Having determined the ground-state structures of H and T phases of pristine Ti_2C monolayers (MD-II and MD-III were selected as ground-state for H and T phases, respectively) we focused on electronic and magnetic properties. Bare MXenes show metallic character with high density of states because of transition metal atoms have *d*- bonding near the Fermi level. Passivated from F, O, OH functional groups, the electronic properties may change dramatically. All calculated electronic band structures are given along the high symmetry direction as Γ, M, K.

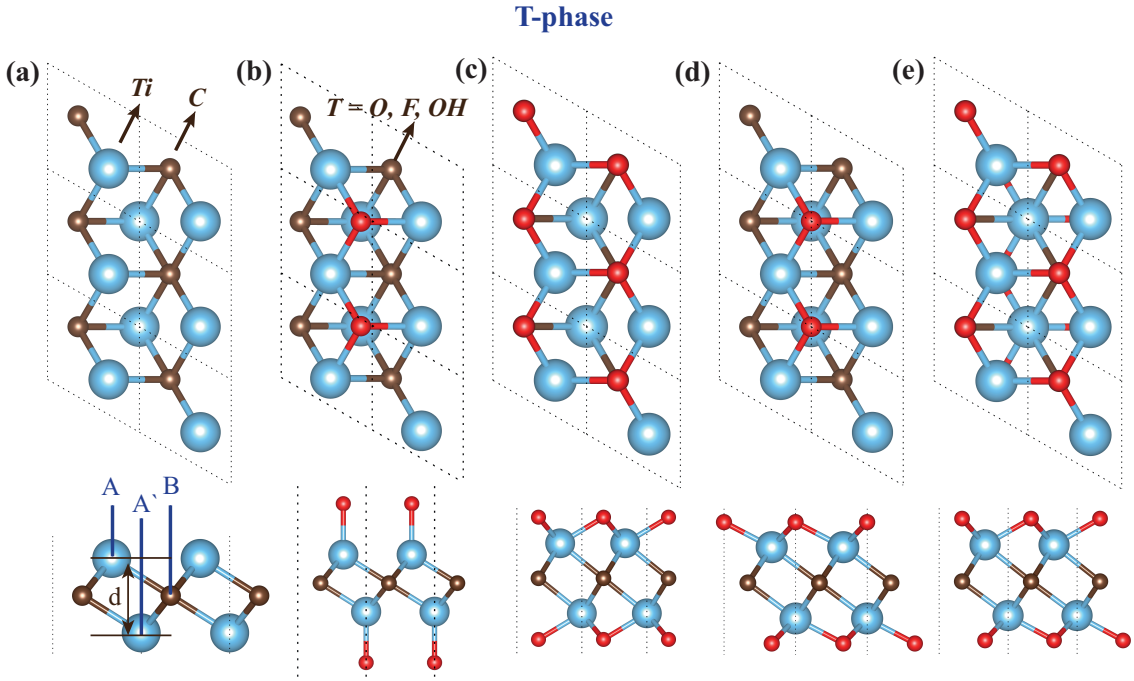

Figure 2. Systematic illustration of T phases of (a) bare Ti_2C and fully terminated functionalization Ti_2CT_2 MXene systems: top and side views of (b) MD-I, (c) MD-II, (d) MD-III, and (e) MD-IV, respectively. Titanium, carbon, and functional groups represented in blue, brown, and red, respectively.

Table 2. Structural parameters and formation energies of MDI–MDIV configurations for pristine T-Ti_2C and chemically functionalized systems.

	Model	Lattice Parameter a (Å)	Thickness d (Å)	Magnetic moment (μ_B)	Formation Energy (eV)
T-Ti_2C		3.08	2.24	1.89	0
T-Ti_2CF_2	MD-I	3.19	2.19	0.00	–12.01
	MD-II	2.97	2.43	0.03	–13.27
	MD-III	3.05	2.29	0.07	–13.83
	MD-IV	3.02	2.35	0.00	–13.61
T-Ti_2CO_2	MD-I	3.03	2.62	0.00	–16.14
	MD-II	2.96	2.77	0.00	–14.37
	MD-III	3.03	2.62	0.00	–16.16
	MD-IV	3.01	2.67	0.00	–15.38
T-$Ti_2C(OH)_2$	MD-I	3.22	2.17	0.00	–9.05
	MD-II	3.01	2.41	0.00	–10.87
	MD-III	3.06	2.32	0.00	–11.21
	MD-IV	3.05	2.35	0.00	–11.07

H phase of pristine Ti_2C shows half-metallic behavior magnetic moments of 2 μ_B per formula unit in Figure 3a. Terminated Ti_2CT_2 (T = F,OH), each F or OH group obtains one electron from Ti_2C turn to metallic character with magnetic moments of 1.27 μ_B and 0.25 μ_B per formula unit, respectively as shown in

Figures 3b and 3d. Oxygen surface termination changes metallic to semiconductor with 0.35 eV band gap value as shown in Figure 3c.

We also investigated T phase of pristine Ti_2C that indicates metallicity with magnetic moments of 1.89 μ_B per formula unit in Figure 4a. We have also tested the magnetic moment and is also verified by the previous studies; 1.91 μ_B per formula unit [26]. F and OH functional group passivations do not change metallic behavior. Magnetic moment of 1.89 μ_B per formula unit vanished when passivated with F and OH. It basically turns to nonmagnetic metallic. Like H phase of pristine Ti_2C, O passivated T phase of pristine Ti_2C changed its electronic properties to semiconductor with 0.25 eV.

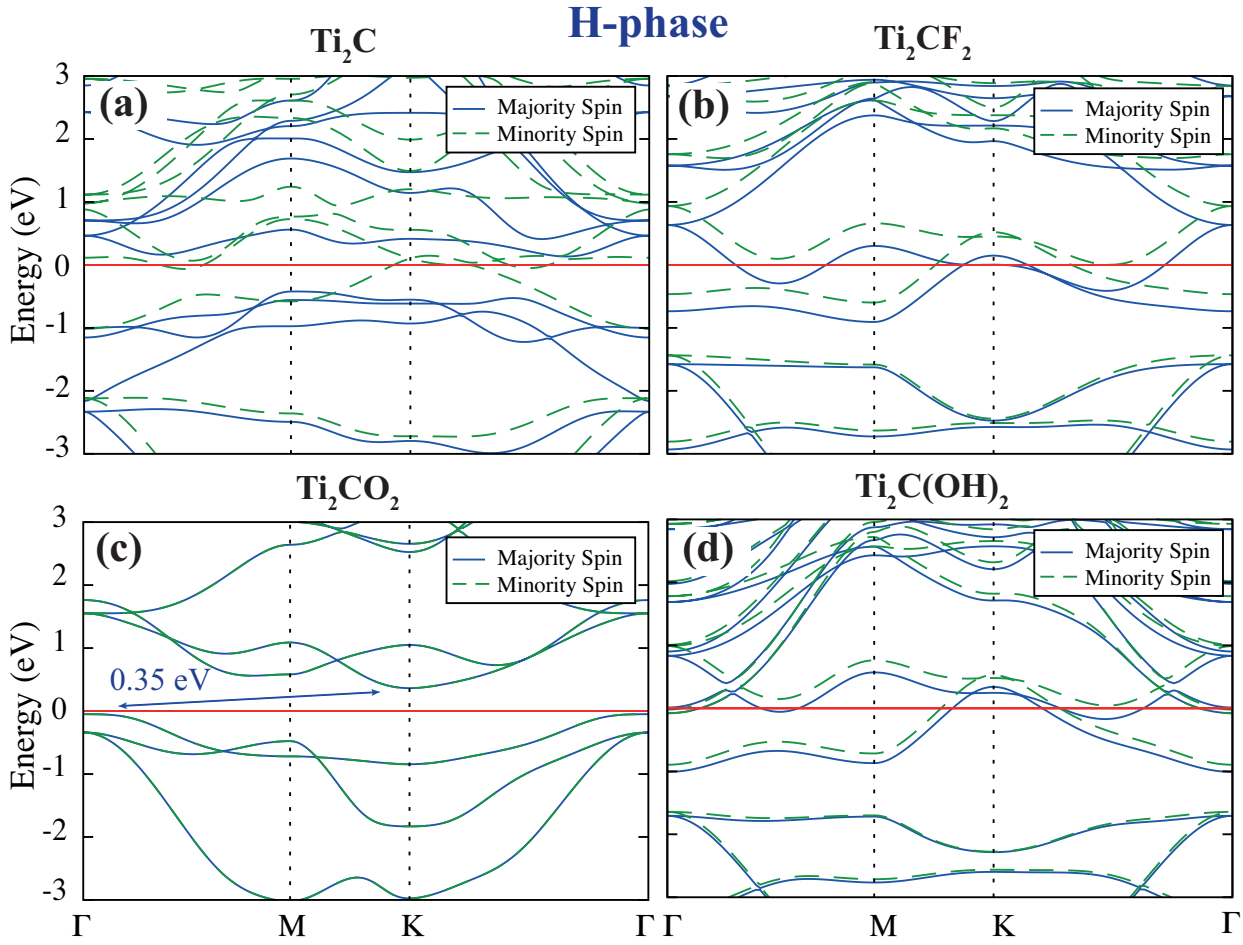

Figure 3. Spin-resolved band structure of H phases of pristine (a) Ti_2C and fully terminated functionalization Ti_2CT_2 as (b) Ti_2F_2 (c) Ti_2O_2 and (d) $Ti_2(OH)_2$ at the equilibrium lattice constants.

4. Summary and concluding remarks

We theoretically investigated the structural, electronic and magnetic properties of both H and T phases of Ti_2C (MXene). We showed for the first time in the literature that Ti_2C changes from being half-metallic to metallic, or to semiconductor in the H phase and being metallic to semiconductor in the T phase, upon surface functionalization. Transition from metal to semiconductor and metal to half-metal in both H and T phases of Ti_2C (MXene) would be interesting issue 2D materials beyond graphene. Nonmagnetic MXenes are also strong candidates for superconductivity due to their display of metallic character.

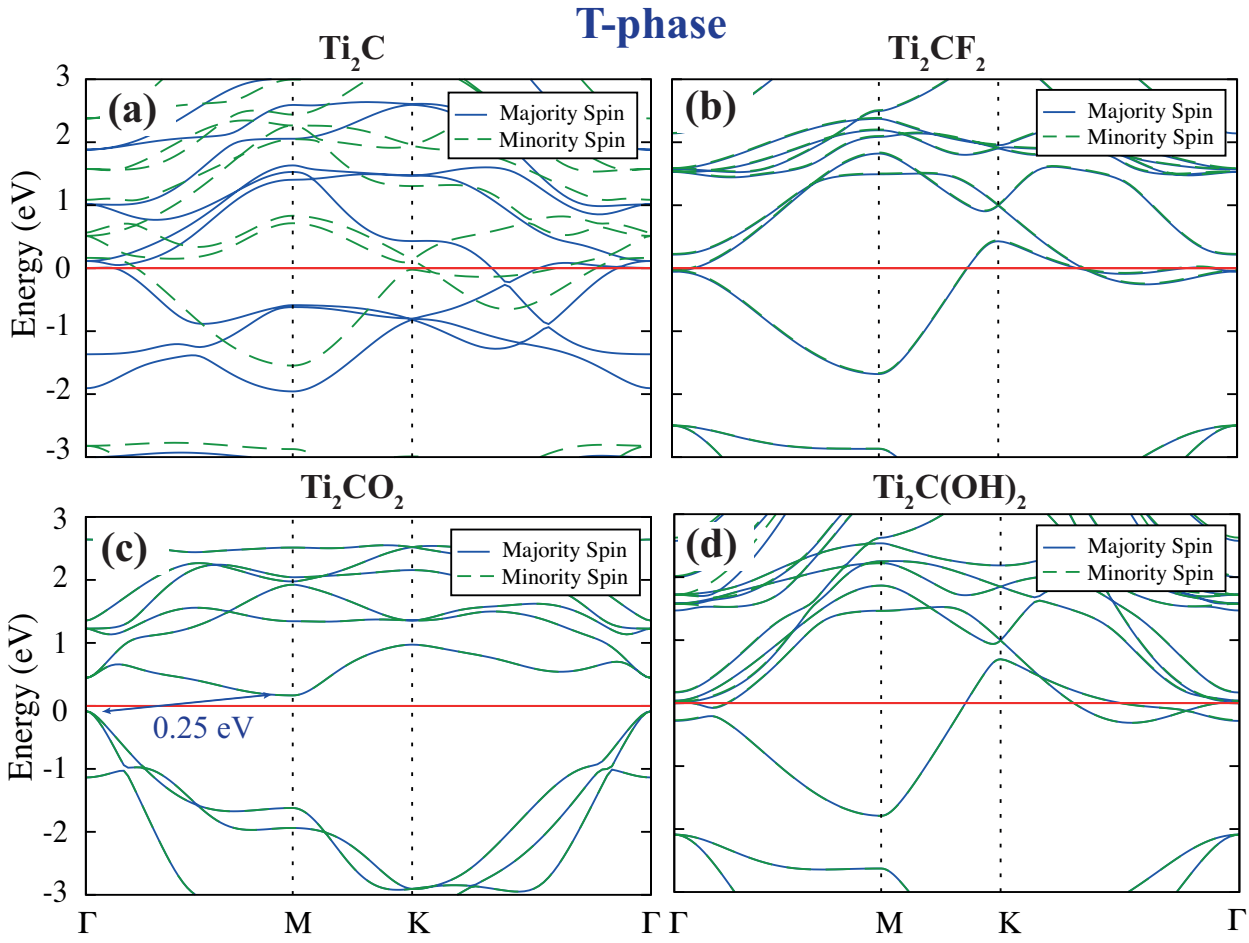

Figure 4. Spin-resolved band structure of T phases of pristine (a) Ti_2C and fully terminated functionalization Ti_2CT_2 as (b) Ti_2F_2 (c) Ti_2O_2 and (d) $Ti_2(OH)_2$ at the equilibrium lattice constants.

Acknowledgments

Computational resources were provided by TÜBİTAK ULAKBİM, High Performance and Grid Computing Center (TR-Grid e-Infrastructure). The author acknowledges financial support the KLU-BAP under the Project Number 189.

References

[1] Novoselov KS, Geim AK, Morozov SV, Jiang D, Zhang Y et al. Electric field effect in atomically thin carbon films. Science 2004; 306 (5696): 666-669. doi:10.1126/science.1102896

[2] Geim AK, Novoselov KS. The rise of graphene. Nanoscience and Technology: A Collection of Reviews from Nature Journals 2010; 11-19. doi:10.1038/nmat1849

[3] Yağmurcukardeş M, Özen S, İyikanat F, Peeters FM, Şahin H. Raman fingerprint of stacking order in HfS_2-$Ca(OH)_2$ heterobilayer. Physical Review B 2019; 99 (20): 205405. doi:10.1103/PhysRevB.99.205405

[4] Kadıoglu Y, Santana JA, Özaydin HD, Ersan F, Aktürk OÜ et al. Diffusion quantum Monte Carlo and density functional calculations of the structural stability of bilayer arsenene. The Journal of Chemical Physics 2018; 148 (21): 214706. doi:10.1063/1.5026120

[5] İyikanat F, Şahin H, Senger RT , Peeters FM. Vacancy formation and oxidation characteristics of single layer TiS3. The Journal of Physical Chemistry C 2015; 119 (19): 10709-10715. doi:10.1021/acs.jpcc.5b01562

[6] Akgenc B. Two-dimensional black arsenic for Li-ion battery applications: a DFT study. Journal of Materials Science 2019; 54 (13): 9543-9552. doi:10.1007/s10853-019-03597-3

[7] Watanabe K, Taniguchi T, Kanda H. Direct-bandgap properties and evidence for ultraviolet lasing of hexagonal boron nitride single crystal. Nature materials 2004; 3(6): 404-409. doi:10.1038/nmat1134

[8] Peng L, Xiong P, Ma L, Yuan Y, Zhu Y et al. Holey two-dimensional transition metal oxide nanosheets for efficient energy storage. Nature communications 2017; 8: 15139. doi:10.1038/ncomms15139

[9] Kolobov AV, Tominaga J. Two-Dimensional Transition-Metal Dichalcogenides 2016; (239) doi:10.1007/978-3-319-31450-1

[10] Wang QH, Kalantar-Zadeh K, Kis A, Coleman JN, Strano MS. Electronics and optoelectronics of two-dimensional transition metal dichalcogenides. Nature nanotechnology 2012; 7 (11): 699. doi:10.1038/NNANO.2012.193

[11] Naguib M, Kurtoglu M, Presser V, Lu J, Niu J, Heon M, Barsoum MW. Two-dimensional nanocrystals produced by exfoliation of Ti_3AlC_2. Advanced Materials 2011; 23 (37): 4248-4253. doi:10.1002/adma.201102306

[12] Urbankowski P, Anasori B, Makaryan T, Er D, Kota S et al. Synthesis of two-dimensional titanium nitride Ti_4N_3 (MXene). Nanoscale 2016; 8 (22): 11385-11391. doi:10.1039/c6nr02253g

[13] Halim J, Kota S, Lukatskaya MR, Naguib M, Zhao MQ et al. Synthesis and characterization of 2D molybdenum carbide (MXene). Advanced Functional Materials 2016; 26 (18): 3118-3127. doi:10.1002/adfm.201505328

[14] Naguib M, Mochalin VN, Barsoum MW, Gogotsi Y. 25th anniversary article: MXenes: a new family of two-dimensional materials. Advanced Materials 2014; 26 (7): 992-1005.

[15] Hantanasirisakul K, Gogotsi Y. Electronic and optical properties of 2D transition metal carbides and nitrides (MXenes). Advanced Materials 2018; 30 (52): 1804779. doi:10.1002/adma.201304138

[16] Lei J, Kutana A, Yakobson BI. Predicting stable phase monolayer Mo_2C (MXene), a superconductor with chemically-tunable critical temperature. Journal of Materials Chemistry C 2017; 5 (14): 3438-3444. doi:10.1039/c7tc00789b

[17] Champagne A, Shi L, Ouisse T, Hackens B, Charlier JC. Electronic and vibrational properties of V_2C-based MXenes: From experiments to first-principles modeling. Physical Review B 2018; 97(11): 115439. doi:10.1103/PhysRevB.97.115439

[18] Si C, Zhou J, Sun Z. Half-metallic ferromagnetism and surface functionalization-induced metal–insulator transition in graphene-like two-dimensional Cr_2C crystals. ACS applied materials & interfaces 2015; 7 (31): 17510-17515. doi:10.1021/acsami.5b05401

[19] Zhang JJ, Dong S. Superconductivity of monolayer Mo_2C: The key role of functional groups. The Journal of chemical physics 2017; 146 (3): 034705. doi:10.1063/1.4974085

[20] Kresse G, Joubert D. From ultrasoft pseudopotentials to the projector augmented-wave method. Physical Review B 1999; 59 (3): 1758. doi:10.1103/PhysRevB.59.1758

[21] Kresse G, Hafner J. Ab initio molecular dynamics for liquid metals. Physical Review B 1993; 47 (1): 558. doi:10.1016/0022-3093(95)00355-X

[22] Perdew JP, Burke K, Ernzerhof M. Generalized gradient approximation made simple. Physical Review Letters 1996; 77 (18): 3865. doi:10.1103/PhysRevLett.77.3865

[23] Kresse G, Furthmüller J. Efficient iterative schemes for ab initio total-energy calculations using a plane-wave basis set. Physical Review B 1996; 54 (16): 11169. doi:10.1103/PhysRevB.54.11169

[24] Grimme S. Semiempirical GGA-type density functional constructed with a long-range dispersion correction. Journal of Computational Chemistry 2006; 27 (15): 1787-1799. doi:10.1002/jcc.20495

[25] Khazaei M, Arai M, Sasaki T, Chung CY, Venkataramanan NS et al. Novel electronic and magnetic properties of two-dimensional transition metal carbides and nitrides. Advanced Functional Materials 2013; 23 (17): 2185-2192. doi:10.1002/adfm.201202502

[26] Gao G, Ding G, Li J, Yao K, Wu M, Qian M. Monolayer MXenes: promising half-metals and spin gapless semiconductors. Nanoscale 2016; 8 (16): 8986-8994. doi:10.1039/c6nr01333c

[27] Zhao S, Kang W, Xue J. Manipulation of electronic and magnetic properties of M2C (M= Hf, Nb, Sc, Ta, Ti, V, Zr) monolayer by applying mechanical strains. Applied Physics Letters 2014; 104 (13): 133106. doi:10.1063/1.4870515